Degradation mechanisms of the ethylene carbonate/diethyl carbonate mixture studied by radiolysis

Furong Wang, Fanny Varenne, Daniel Ortiz, Valentin Pinzio, Mehran Mostafavi, Sophie Le Caer

Degradation by ionizing radiation of the ethylene carbonate/diethyl carbonate mixture

Furong Wang,[a] Fanny Varenne,[b] Daniel Ortiz,[b] Valentin Pinzio,[b] Mehran Mostafavi,[a] Sophie Le Caër*[b]

[a] F. Wang, Pr. M. Mostafavi
Laboratoire de Chimie-Physique/ELYSE, UMR 8000 CNRS/UPS
Université Paris Sud, Bât. 349, F-91405 Orsay Cedex, France

[b] Dr F. Varenne, Dr D. Ortiz, V. Pinzio, Dr S. Le Caër
LIONS, NIMBE, UMR 3685, CEA, CNRS, Université Paris-Saclay, CEA Saclay, Bât. 546
F-91191 Gif-sur-Yvette Cedex, France
E-mail: sophie.le-caer@cea.fr

Abstract

The reactivity of ethylene carbonate (EC) and of the ethylene carbonate/diethyl carbonate (DEC) mixture is studied under ionizing radiation in order to mimic aging phenomena occurring in lithium-ion batteries. Picosecond pulse radiolysis experiments show that the attachment of the electron on EC molecule is ultrafast ($k(e^-_{EC} + EC) = 1.3 \times 10^9$ L mol^{-1} s^{-1} at 46°C). This reaction rate is accelerated by a factor of 5.7 as compared to the one of the electron attachment in propylene carbonate, implying that the presence of the methyl group significantly slows down the reaction. In the case of the 50/50 EC/DEC mixture, just after the electron pulse, the electron is solvated by a mixture of EC and DEC molecules, but its fast decay is attributed to the electron attachment on the EC molecule exclusively. Stable products detected after steady-state irradiation include mainly H_2, CH_4, CO and CO_2. The evolution of the radiolytic yields with the EC fraction shows that H_2 and CH_4 do not exhibit a linear behavior, whereas CO and CO_2 obey it. Indeed, H_2 and CH_4 mainly arise from the excited state of DEC, whose formation is significantly affected by the evolution of the dielectric constant of the mixture and by the electron attachment on EC. CO formation is mainly due to the reactivity of the EC molecule that is not affected in the mixture as proven by pulse radiolysis experiments.

1. Introduction

Among power sources, Lithium-ion batteries (LIB) are efficient energy storage devices suitable for portable electronics applications.[1, 2] Moreover, they are the most promising systems for fields such as electric vehicles or stationary energy storage as they display high energy density and low self-discharge.[3] LIBs are complex systems, hence the understanding of their behavior concerns different research areas such as material, surface and electrochemical science. Thus, their basic study is challenging and the studies of ultrafast and fast reactions to understand the mechanisms of the degradation are unavoidable.

LIBs generally consist in a carbonaceous anode and a transition meal oxide cathode. Commercial electrolytes are usually composed of a conducting salt such as lithium hexafluorophosphate ($LiPF_6$) dissolved in a mixture of linear (low dielectric constant and low viscosity) and cyclical (high dielectric constant and high viscosity) carbonates. A separator soaked in the electrolyte is located between the electrodes for the charge transfer of Li^+ ions. Mixing solvents of different nature allows providing electrolytes with low viscosity for ion transport and high dielectric constant in order to dissolve the salt.[4]

Aging phenomena significantly reduce the cycle life of LIBs and lead to the production of hazardous compounds. Indeed, the formation of hydrofluoric acid[5] and dihydrogen has been reported in several works[6]. The stability of the electrolyte has been identified as one of the key points of aging phenomena.[7] That is why the understanding these phenomena is a crucial issue to provide highly durable and safe LIBs under normal and abusive conditions. The degradation of the electrolyte often cannot be investigated by usual thermally activated aging methods explaining that these studies may be costly, lengthy and usually qualitative.[8]

Recently, we demonstrated that radiolysis (i.e., the chemical reactivity induced by the interaction between matter and ionizing radiation) provides an elegant solution to these issues, as it is a powerful tool for a short-time identification (minutes-days, so it strongly accelerates aging processes) of the products occurring from the degradation of a LIB electrolyte after several weeks-months of cycling.[9-11] Indeed, we have shown that the highly reactive species created in the irradiated solution are the same as the ones obtained during the charging of a LIB using similar solvents. Having worked on pure carbonate solvents (diethyl carbonate and propylene carbonate, with/without $LiPF_6$),[9-11] the purpose of the present work is to use radiolysis to investigate now the properties of a mixture of a linear (non-polar) and cyclical (polar) carbonate. Indeed, a mixture of ethylene carbonate and diethyl carbonate is more

complex, more realistic and representative of the solvents used in LIBs. We will benefit here from the possibility of radiolysis to probe the reactivity on very large timescales, i.e. at the picosecond timescale to evidence the first stages of the matter/ionizing radiation interaction and at long times to identify, and when it is possible, quantify, the main species produced upon steady-state irradiation.

Material and methods

Chemicals

Ethylene carbonate (EC), diethyl carbonate (DEC) were provided by Sigma-Aldrich (anhydrous grade, purity > 99 %) and were used without further purification. Electrolytes were prepared under water-free pure argon atmosphere in a glove box. For the long time scale radiolysis experiments, around 1 mL of each electrolyte was introduced in a glass ampoule and degassed by argon bubbling for 30 min. Then, the ampoule was thrice degassed and filled with pure argon 6.0 at 1.5 bar.

Solid at ambient temperature, EC was slowly heated in a bath water set at 38°C before preparing electrolytes. After the long time scale irradiation, EC was heated again gently to allow any gas which may be trapped in the solid phase to be released in the gas phase and also to be able to perform analysis in the liquid phase. We checked carefully that heating non-irradiated EC under exactly the same conditions did not lead to the release of any gas.

The main carbonate compounds cited in the present work are represented in Scheme 1.

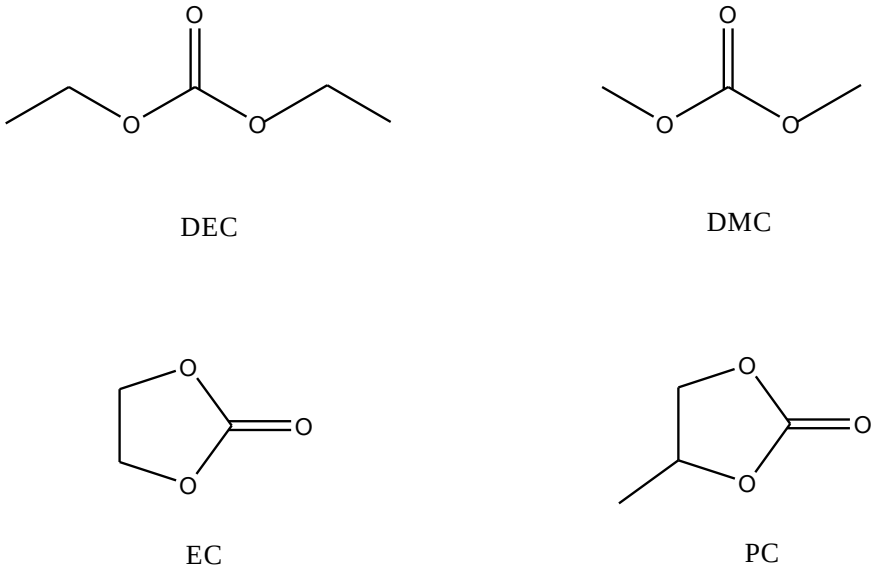

Scheme 1. Chemical structures of diethyl carbonate (DEC), dimethyl carbonate (DMC), ethylene carbonate (EC) and propylene carbonate (PC).

The physicochemical properties of EC, DEC and the 50/50 (in volume) EC/DEC mixture are given in Table 1. In this mixture, the EC molar fraction is 0.57. Unless otherwise specified, EC/DEC refers to the 50/50 (in volume) mixture.

Table 1. Physicochemical properties of carbonates and their mixture.[4] *: present work.

Property	EC	DEC	EC/DEC
ρ (g mL^{-1})	1.321 at 25°C	0.969 at 25°C	1.16 ± 0.01 at 25°C*
State at 20°C	Solid	Liquid	Liquid
Melting temperature (°C)	36.4	- 74.3	
Boiling temperature (°C)	248	126	
Viscosity (mPa.s)	1.90 at 40°C	0.75 at 25°C	1.64 ± 0.03 at 25°C*
Dielectric constant	90.03 (40°C)[12]	2.82 at 25°C[13]	

Concerning now various EC/DEC mixtures, the corresponding dielectric constants are not available in the literature, but insights can be gained by considering the dielectric constants measured in the EC/DMC (dimethyl carbonate) mixtures, as DMC is very similar to DEC (Table 2).[12]

Table 2. Evolution of the dielectric constant in the EC/DMC mixture at 40°C as a function of the molar fraction (x) of EC.[12]

xEC + (1-x)DMC	Dielectric constant (40°C)
0	3.19
0.2	10.27
0.4	23.24
0.6	40.62
0.8	62.43
1	90.03

Picosecond pulse radiolysis experiments

The ultrafast kinetics of the solutions was accessed by picosecond pulse radiolysis with the laser-driven electron accelerator ELYSE.[14, 15] A pump-probe setup installed at the experimental area 1 was used whose basic optical configuration and data acquisition scheme are described in references [14, 15]. The transient absorbance of the samples was probed in a flow cell with 5 mm nominal optical path collinear to the electron pulse propagation. The electron pulses were delivered with pulse duration of about 7 ps and electron energy of 7.6 MeV at a repetition rate of 10 Hz. The broadband pump-probe system was operated using a single crystal of yttrium aluminum garnet (YAG) for continuum light generation optimized in the NIR.[16] Both probe and reference beams were coupled into an optical fiber, transmitted to an adapted spectrometer, and dispersed onto the specific line scan detectors. For the measurements in the NIR, a customized broadband polychromator with an InGaAs photodiode array from Hamamatsu (G11608-512DA) was used.[16] The dose per pulse was deduced from the absorbance of the hydrated electron e^-_{aq} in water, measured just before a series of experiments. The dose was then derived from the yield at 15 ps: $G(e^-_{aq})_{15\,ps} = 4.25 \times 10^{-7}$ mol J^{-1} and from the molar absorption coefficient $\varepsilon_{800\,nm} = 1.53 \times 10^4$ L mol^{-1} cm^{-1}.[17] The dose per pulse in water was then around 47 Gy. In all irradiation experiments, and according to the stopping powers in the carbonates and in water, the dose received by the solution and by water was considered to be the same.

Irradiation experiments for the identification of formed stable products

Irradiation experiments to identify the products generated in the gas phase were performed with a Gammacell 3000 ^{137}Cs source. The dose rate determined using the aqueous Fricke dosimeter[18] was 5.0 Gy.min^{-1} (1 Gy = 1 J.kg^{-1}) and the highest dose achieved was around 20 kGy.

Products formed in the gas phase

The degradation products formed in the gas phase, after irradiation at a dose of 20 kGy, were identified by gas chromatography (Agilent, 6890 GC) hyphenated to a mass spectrometer equipped with an electron impact source (EI) and a quadrupole mass analyzer (Agilent, 5973 MS). The products were separated with a (25 m x 0.32 mm) CP-PorabondQ column provided by Varian. Helium was used as vector gas with a flow rate set at 2 mL min^{-1}. The temperature of the injector was fixed at 110°C in splitless mode. The separated products were fragmented at 70 eV and detected within mass range from 4 to 160 *m/z*. The identification of the products was performed by comparing the experimental spectra to the NIST mass spectra library. The main produced gases i.e. H_2, CH_4, CO and CO_2 were quantified by gas chromatography (µ-GC R3000, SRA Instruments) with helium as a carrier gas. More experimental details are given in [9].

2. Results and discussion

Picosecond pulse radiolysis experiments of EC, DEC and of the EC/DEC mixture

With the requirement to renew the sample, all pulse radiolysis experiments were performed at 46°C well above the melting temperature of EC (36.4°C, see Table 1). The transient optical absorption spectra detected at 46°C after the electron pulse in neat DEC, neat EC and in the 50/50 EC/DEC mixture are given in Figure 1. The corresponding kinetics is given in the insets. In DEC, the absorption band increases monotonously until the detection limit (Figure 1a). The band observed for DEC solution at 46 °C (Figure 1a) is similar to the one detected in neat DEC at room temperature.[19] It was assigned to the formation of the solvated electron.[19] Usually, a red shift of the absorption band occurs when increasing the temperature,[20] but the maximum of the absorption band is out of our spectral window. The maximum of the transient absorption band is found at 1250 nm and at 1410 nm in the case of EC (Figure 1b) and EC/DEC mixture (Figure 1c), respectively. Due to the fact that EC and DEC are both carbonates, we assume that the mixture is homogeneous on a microscopic scale, i.e. that EC

and DEC molecules are completely mixed together. In the case of PC, a cyclical carbonate similar to EC (see Scheme 1), a broad absorption band with a maximum at 1360 nm was detected just after the electron pulse. This band was attributed to the solvated electron.[21] In the present case, and similarly to the case of PC, the band with a maximum at 1250 nm is also attributed to the solvated electron. Considering now the mixture (Figure 1c), the broad band with a maximum at 1410 nm can be assigned to the solvated electron. Our observation is in agreement with the fact that in the case of a homogeneous mixture, the absorption band of the solvated electron is usually ranging between the two maxima of the absorption band of each solvent, as already observed in the case of the THF/H_2O mixture which also contains a weakly polar and a strongly polar compound.[22, 23] In this case, and for a molar fraction of THF lower than 0.49, the presence of THF only slightly changed the spectrum of the solvated electron, that was similar to the spectrum of the solvated electron in water, but at a higher temperature.[23] In our case, the transient spectrum we measure (for a molar fraction of DEC equal to 0.43) is similar to that obtained in EC, but red-shifted (Figure 2). Contrary to the measurements performed in THF/water mixtures where time-resolved spectra exhibited isosbestic points, and where the hydration dynamics was thus described by a two-state kinetics, implying that nanometer inhomogeneities exist in these mixtures, no such trend is evidenced here (Figure 1c), suggesting that the EC/DEC mixture is homogeneous, even at the molecular scale.[24] The band of the solvated electron in EC/DEC is broader than the one measured in neat EC as clearly evidenced on the spectrum measured 20 ps after the electron pulse (Fig. 2). This strongly suggests that solvated electrons surrounded by DEC and EC molecules are formed in the mixture. The kinetics given in the insets of Figure 1 illustrate also the different behaviors. Whereas the decay of the solvated electron is slow in DEC, it is ultra-fast in EC and in the EC/DEC mixture.

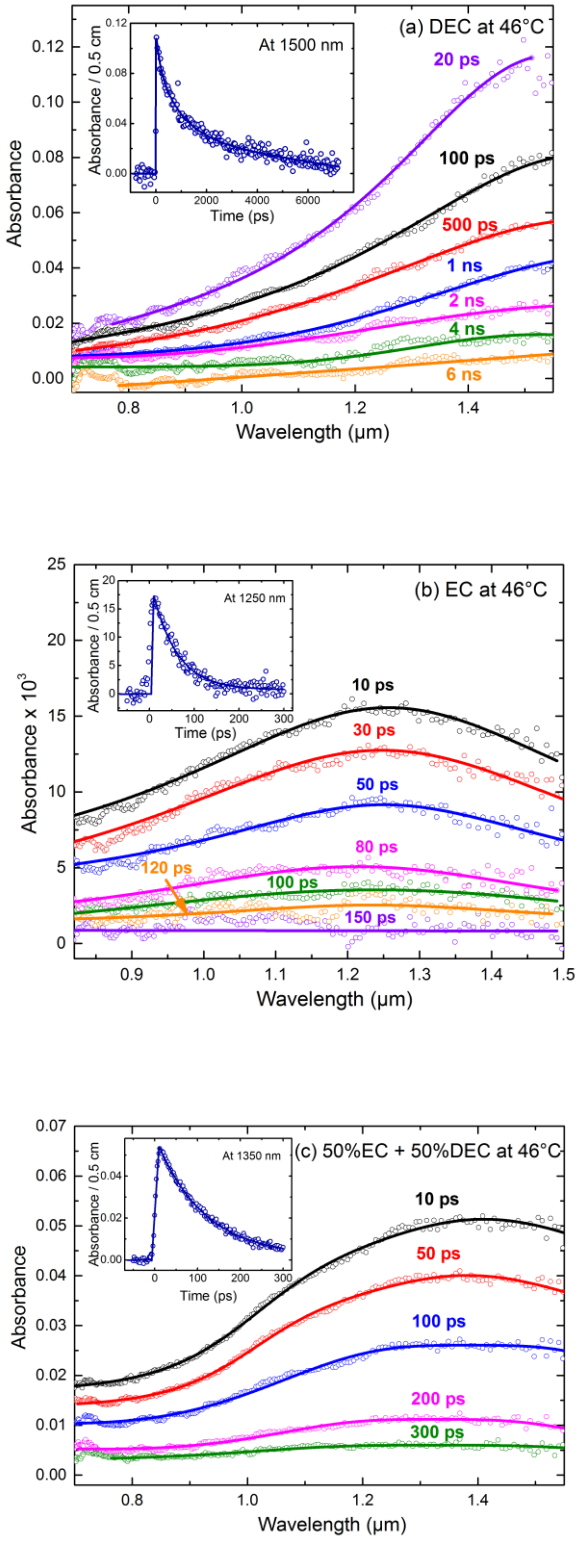

Figure 1. Transient optical absorption spectra in (a) DEC; (b) EC and (c) 50/50 EC/DEC mixture after the picosecond electron pulse (dose per pulse: 47 Gy). Kinetics is given in the

insets. All experiments were performed at 46°C. The points are the experimental data and the lines are a guide for the eyes.

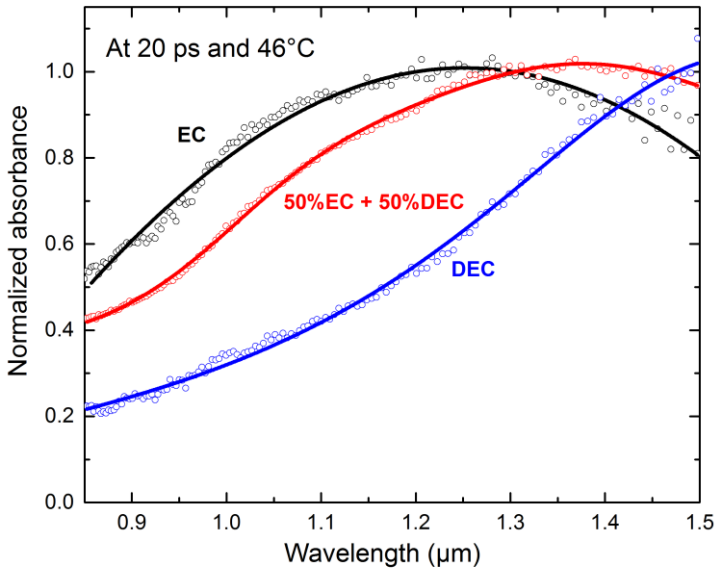

Figure 2. Normalized spectra, measured at 46°C, of the solvated electron in EC (black), DEC (blue) and 50/50 EC/DEC (red) measured 20 ps after the electron pulse. The circles are the experimental points and the lines are a guide for the eyes.

It is well known that the primary effects of radiation on a molecule M are ionization and excitation:

$M \rightarrow M^*, M^{\bullet+}, e^-$ (1)

The normalized absorbance decays at 46°C for various carbonates (DEC, PC, EC and 50/50 EC/DEC) is represented in Figure 3a.

Contrary to DEC, the decay of the solvated electron in PC is complete within 2 ns. This was previously attributed to reaction (2) corresponding to the attachment of the solvated electron on PC, leading to the formation of the radical anion:

$e^-_{PC} + PC \rightarrow PC^{\bullet-}$ (2) $k(e^-_{PC} + PC) = 1.9 \times 10^8$ L mol^{-1} s^{-1} at room temperature.[21]

Indeed, the decay obeys a pseudo first-order law, and the fast decay of the solvated electrons cannot be due to reactions within the spurs. Moreover, in a neat solvent, the sole abundant species is the solvent itself. At 46°C, the density of propylene carbonate is 1.18 g cm^{-3}.[25] The concentration of PC being 11.6 mol L^{-1}, $k(e^-_{PC} + PC) = 2.3 \times 10^8$ L mol^{-1} s^{-1} at 46°C. A slight acceleration between ambient temperature and 46°C is clearly observed.

In the case of EC, the same interpretation holds. The decay is ultrafast and obeys a pseudo first-order law (Figure 3a). Interestingly, it is significantly faster in EC than in PC. In ethylene carbonate, the density was measured to be 1.32 g cm^{-3} at 36°C and calculated to be 1.29 g cm^{-3} at 52°C.[26] Assuming that the density of EC is 1.30 g cm^{-3} at 46°C, then we find, for an EC concentration of 14.8 mol dm^{-3}:

e^-_{EC} + EC → $EC^{\bullet -}$ (3) $k(e^-_{EC} + EC) = 1.3 \times 10^9$ L mol^{-1} s^{-1} at 46°C.

Hence, the presence of the methyl group slows down the rate constant of the electron attachment by a factor of 5.7. This can be attributed to steric hindrance by the methyl group as well as to its electron donating effect by induction.

Noteworthy, in the case of PC, a shift of the absorption band was observed during the first 50 ps. It was attributed to the solvation of the electron. In the present case, we did not observe any shift of the absorption band. This can be due to the higher temperature favoring faster solvation of the solvent and also to the very fast decay of the solvated electron. Let's also point out that the maxima of the bands (1310 nm after 50 ps in PC at room temperature and 1250 nm in EC at 46°C) are very close to each other, indicating that the structure of electrons solvated in PC and in EC are similar, as expected.

In polar solvents, the electron radiolytic yield at 10 ps ($G_t(e^-_{EC})$) is generally about 4×10^{-7} mol J^{-1}.[27, 28] Knowing that $\varepsilon_\lambda = A_{\lambda,t}/(D \times \rho \times l \times Gt(e^-_{EC}))$, where ε_λ is the molar absorption coefficient of the solvated electron expressed in L mol^{-1} cm^{-1}, $A_{\lambda,t}$ is the measured absorbance at 1250 nm, D is the dose (47 J kg^{-1}), ρ is the density of the solution (1.30 kg L^{-1}) and l is the optical path in cm, $\varepsilon_{1250\,nm}(e^-_{EC})(10\ ps)$ is calculated to be 1300 L mol^{-1} cm^{-1}. This value is too small to be possible,[29] meaning that the electron radiolytic yield at 10 ps is much smaller than that postulated above (4×10^{-7} mol J^{-1}). As we showed in the case of PC, and even more striking for EC, the major part of pre-solvated electrons gives then radical anions $EC^{\bullet -}$, and only a small population of electrons leads to the formation of solvated electrons that will then form radical anions according to (3). The same calculation can be performed in the case of the EC/DEC mixture and leads to a too small value of the molar extinction coefficient at its maximum (4000 L mol^{-1} cm^{-1}). This also implies that presolvated electrons preferentially react with EC, forming $EC^{\bullet -}$, in the EC/DEC mixture.

The decay kinetics measured in the DEC/EC mixture is similar, although slower, as the one measured in EC (Figure 3a). It also obeys a pseudo first-order law. This means that the decay in DEC/EC is attributed to the attachment of the solvated electron exclusively on the EC molecule. In fact, DEC is a non-polar solvent and the diffusion of the solvated electron in this kind of solvent is very fast. The solvation energy of the electron in nonpolar solvent is low

and the electron can move from one cavity to another one very quickly.[30-32] Therefore, the electron can be very quickly trapped by EC molecules which are in contact with DEC molecules to form $EC^{\bullet -}$. The slower decay of the solvated electron in EC/DEC solution compared to that in EC is due to the fact that the EC concentration is of course lower in the mixture than in the neat solvent. At 46°C, the density of DEC is equal to 0.95 g cm^{-3}.[33] The density of the mixture at 46°C is measured to be 1.14 g cm^{-3}. This implies that, in the EC/DEC mixture:

$e^-_{EC/DEC}$ + EC → $EC^{\bullet -}$ (4) at 46°C, $k(e^-_{EC/DEC} + EC) = 1.4 \times 10^9$ L mol^{-1} s^{-1} which is almost the same value as the one determined in neat EC (3).

At room temperature (Figure 3b), with a mixture density of 1.16 g cm^{-3} (Table 1), we find:

$e^-_{EC/DEC}$ + EC → $EC^{\bullet -}$ (4) at room temperature, $k(e^-_{EC/DEC} + EC) = 1.2 \times 10^9$ L mol^{-1} s^{-1}, which is 6.3 times higher than the value measured in PC at the same temperature. The effect of temperature on the rate constant is small and similar in PC and EC, in the studied temperature range (Figure 3b).

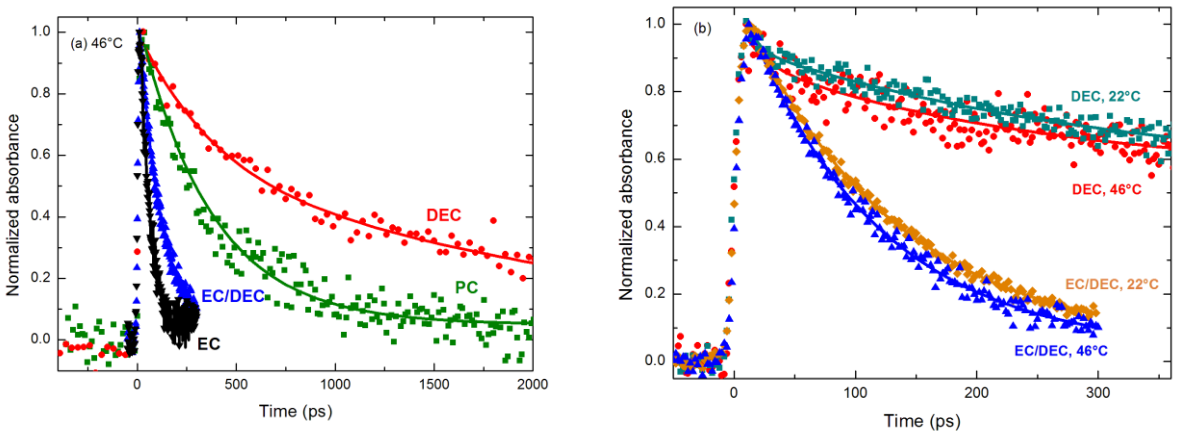

Figure 3. (a) Normalized decay kinetics at 46°C of the solvated electron in DEC (red circles), PC (green squares), EC (black down triangles) and EC/DEC (blue up triangles); (b) comparison of the normalized decay kinetics at 46°C and at room temperature (22°C). The lines guide the eyes.

Last, if the solvated electron is formed in DEC, it will react very quickly in EC or in the EC/DEC mixture with EC to form the radical anion $EC^{\bullet -}$ (Scheme 2).

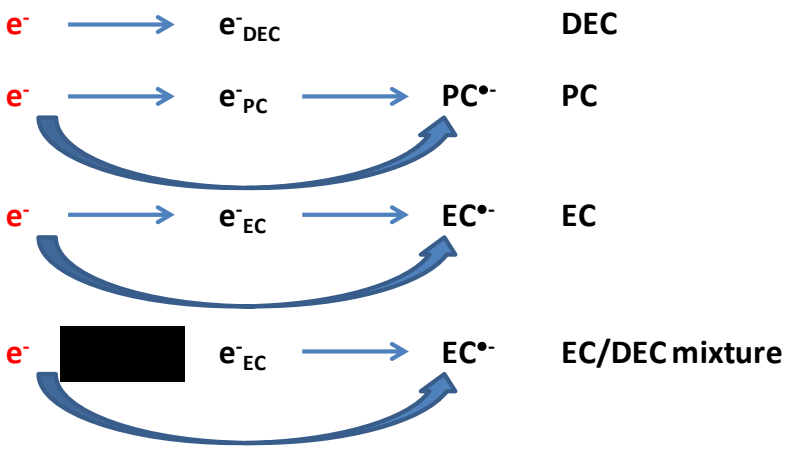

Scheme 2. Scheme illustrating the first reductive processes occurring in DEC (a linear carbonate), in two cyclical carbonates (PC and EC) and in the EC/DEC mixture.

Composition of the gas phase after irradiation

Products formed in the gas phase in the EC/DEC mixture upon γ-irradiation are presented in Figure 4. Different types of stable products are detected including alkanes and oxygenated molecules such as esters, ethers and aldehydes. Irradiation of the mixture shows the formation of molecules that are found in irradiated DEC (alkanes such as C_3H_8 and C_4H_{10}, ether such as $C_2H_5OC_2H_5$)[9]. Moreover, similar molecules were identified by GC-MS of the EC-DMC/$LiPF_6$ electrolyte recovered from the cycled stainless steel/Li cell at 55°C:[34] CH_3OCH_3 (here $C_2H_5OC_2H_5$ with DEC instead of DMC), CH_3OCHO (here C_2H_5OCHO with DEC instead of DMC)…. Even though H_2, CH_4 and CO molecules are not detected by GC-MS (Figure 4), they are indeed the main molecules produced upon irradiation, as evidenced by mass spectrometry with electron ionization (EI/MS). They are detected and quantified by µ-GC. The quantification by mass spectrometry (EI/MS) of all the compounds formed upon irradiation is difficult, as many species are formed and lead to the same fragmentation ions. Therefore we quantified only the main gases (H_2, CO, CO_2, CH_4) that are measured directly by µ-GC. C_2H_6 is also produced in significant amounts, but cannot be quantified by µ-GC.

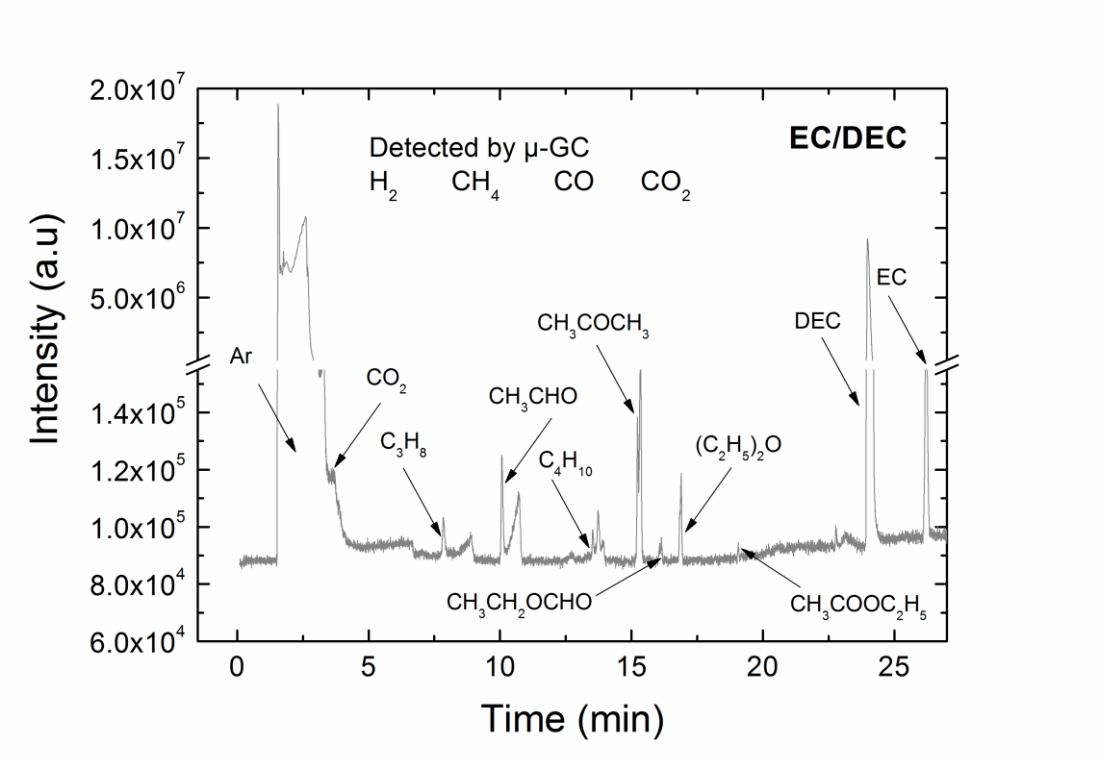

Figure 4. Gas decomposition products of EC/DEC identified by GC-EI/MS after γ-irradiation at 20 kGy. The formation of acetone can be due to washing and not to irradiation.

For each gas (H_2, CH_4, CO and CO_2), the amount produced increases linearly with the dose as shown in Figure 5. The corresponding radiolytic yields defined as the amount of gas produced per energy unit, expressed in μmol.J^{-1}, are deduced from the slope of the lines. The results are given in Table 3. For neat EC, the major gases produced are CO_2 and CO as compared to H_2 and CH_4, which is negligible. In the case of DEC, the major gases produced upon irradiation are H_2 and CO_2 (Table 3). For the EC/DEC mixture, the major gas formed is CO_2 as compared to CO and H_2. CH_4 is produced in lower amount than the other gases.

In the case of EC, the CO_2 radiolytic yield is twice the radiolytic yield of CO, contrary to the case of PC for which these two yields were equal.[11] In this latter case, $PC^{\bullet+}$ and $PC^{\bullet-}$, both produced in the same amounts, lead respectively to the formation of CO_2 and CO.[11] This is obviously no longer the case for EC. Nevertheless, $EC^{\bullet+}$ and $EC^{\bullet-}$ are produced in the same amounts but the differences in the CO and CO_2 yields show that both gases can be produced thanks to the oxidative and reductive pathways. This is in agreement with electrochemistry experiments. Indeed, it was shown that in the oxidation pathway, the radical cation $EC^{\bullet+}$ leads, after ring opening, to the $^{\bullet}OCH_2CH_2OC^{\bullet+}O$ intermediate. It will then form mainly CO_2, but also CO when working at high potential.[35] Let's point out that the nature of the oxidant

($EC^{\bullet+}$) in cyclical carbonates is still under debate. Very recently, Borovkov[36] proposed, in the case of PC, that the radical cation consists in fact of ionized complex molecules having opposite orientations of the carbonyl groups. Lastly, according to electrochemistry experiments, both molecules can be generated from the radical anion in the reductive channel,[37] but CO arises mainly from this pathway.

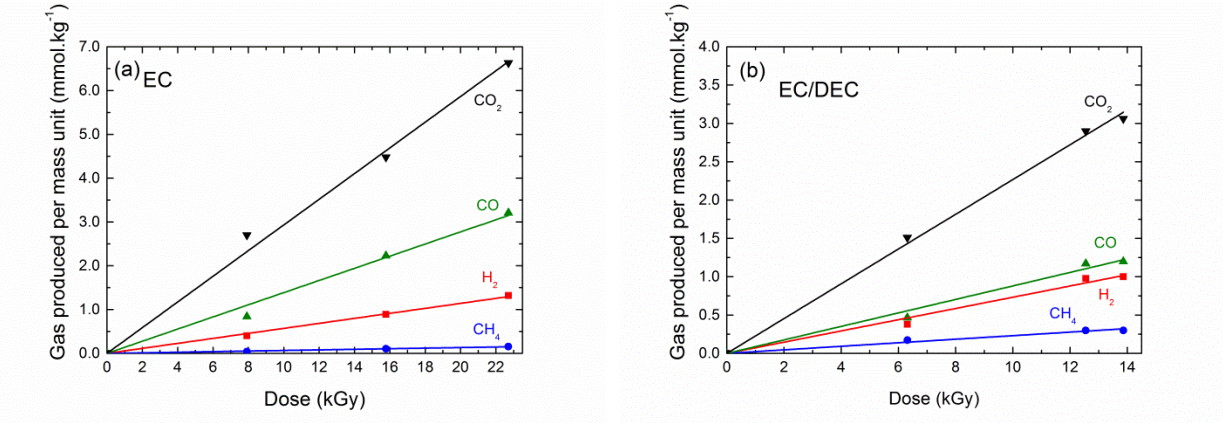

Figure 5. Evolution of the main decomposition products formed in the gas phase and measured by µ-GC after γ-irradiation of EC (a) and EC/DEC (b) as a function of the dose.

Table 3. Radiolytic yields (in µmol J^{-1}) of the main decomposition gases determined by µGC*. The results obtained for DEC comes from reference [9].

Gas	EC	EC/DEC	DEC[9]
H_2	0.06	0.07	0.13
CH_4	< 0.01	0.02	0.08
CO	0.14	0.09	0.05
CO_2	0.29	0.23	0.21

*The uncertainty bars are estimated to 10 %.

When a mixture of compounds is irradiated, then the fraction of the total absorbed energy transferred to each compound is proportional to the weight fraction of the compound and to the mean mass collision stopping power of the compound for the various ionizing particles present in the medium. The latter term is generally assumed to be proportional to the *Z/A* ratios of the compounds, with *Z/A* the ratio of the atomic number to the atomic mass number of the compound.[38] From this, it follows that:

$G(P) = \sum_i G(P)_i f_i$ (5)

with *G(P)* the radiolytic yield of the product P formed in a mixture, $G(P)_i$ the radiolytic yields of P from the compound *i* in the mixture and f_i the electron fraction of *i*. This equation is generally referred as the "mixture law", although it is a simple approximation.

Moreover, $f_i = \omega_i \frac{(\frac{Z}{A})_i}{(\frac{Z}{A})_{mixt}}$ (6)

with ω_i the weight percentage of compound *i*, and $(\frac{Z}{A})_{mixt} = \sum_i \omega_i (\frac{Z}{A})_i$.

In the present case, the *Z* values for DEC and EC are 64 and 46 respectively, whereas the *A* values are 118 and 88, respectively. The evolution of the H_2, CH_4, CO and CO_2 yields as a function of the electron yield in EC, for various EC/DEC mixtures is represented in Figure 6. Let's point out that in all the mixtures studied, the radiolytic yields range between the values measured for pure DEC and pure EC.

In Figure 6, the straight lines represent the expected yields if Eq. (5) is obeyed. Noteworthy, in most cases, this mixture approximation, which assumes that the behavior of excited and ionized species produced and their reaction products are not changed by the presence of the other compounds, is not followed. This is obviously not the case for H_2 and CH_4 (Figures 6a and 6b). Indeed, in this case, these two gases are mainly produced from the excited state of DEC.[9] In DEC, which is a solvent with a very low dielectric constant (2.82, see Table 1), the recombination of $DEC^{\bullet+}$ with the electron is highly favored, leading to the formation of DEC*.[9] This excited molecule will then lead to H_2 and CH_4 (Table 3). In the EC/DEC mixture, picosecond pulse radiolysis experiments suggest that the pre-solvated electron will preferentially attach to EC, than react with $DEC^{\bullet+}$, decreasing then the amount of DEC*. Therefore, the reaction pathways leading to H_2 and CH_4 are no longer so much favored. Moreover, the mixture becomes more and more polar by increasing EC and the probability of excited state formation becomes less likely (Table 2).

The situation is clearly different for the CO and CO_2 gases (Figures 6c and 6d). In these latter cases, the system roughly obeys the mixture law, but for different reasons. The CO formation is mainly due to EC, and to DEC in a lower extent (Table 3). Picosecond pulse radiolysis experiments evidence that, in the case of mixtures, the solvated electron will react with EC (Figure 3a), forming the radical anion (reaction 4) that will then generate CO and CO_2. Therefore, in the case of CO, a crude linear behavior of the radiolytic yield with the electron fraction in EC is expected, as the reaction pathway leading to its formation is not affected by the mixture.

The case of CO_2 is more complex, as it has different origins. Indeed, it arises from $EC^{\bullet+}$, from $EC^{\bullet-}$, but also from DEC*, $DEC^{\bullet+}$,[9] and, as suggested by EPR experiments, after reaction of the pre-solvated electron with DEC followed by dissociative electron attachment.[39] Clearly, the DEC* and the dissociative electron attachment channels are affected by the mixture. We suppose here that the linear behavior we observe in the CO_2 case (Figure 6d) is rather due to the fact the CO_2 radiolytic yields measured in DEC and in EC are close to each other, making a weak linear dependency, which will be not affected by the mixture due to compensating factors.

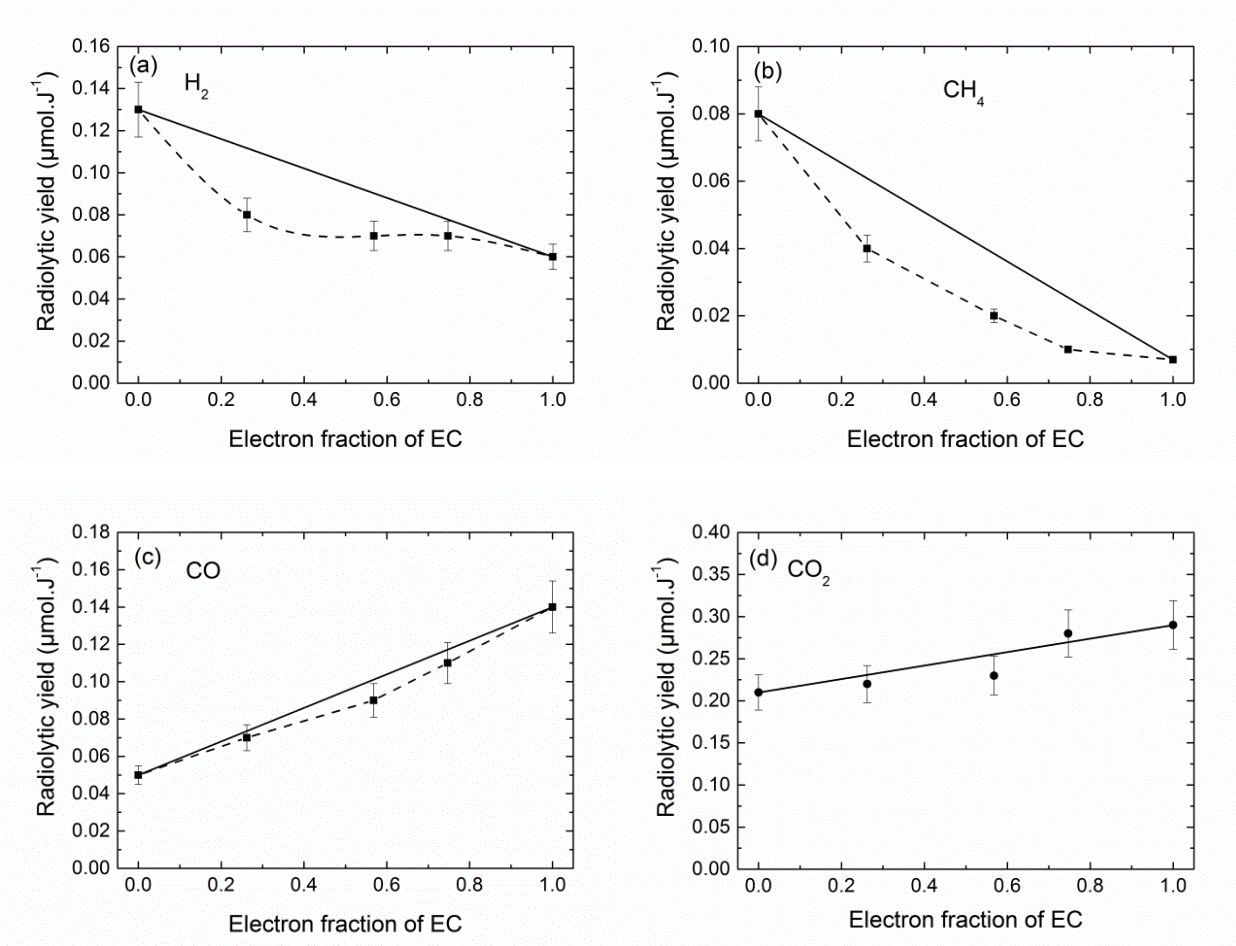

Figure 6. Effect of the EC electron fraction on the radiolytic yields of the main decomposition gases quantified by µGC. (a) H_2; (b) CH_4; (c) CO; (d) CO_2.
The uncertainty bars are estimated to 10 %.

Last, the products formed in the liquid phase in the irradiated 50/50 EC/DEC mixture and investigated by means of High Resolution Mass Spectrometry are given in Supporting

Information. These products are: i) typical of irradiated EC; ii) typical of irradiated DEC; iii) due to the presence of the two compounds in the mixture such as dicarbonate, carbonate with two ether functions, and carbonate with ether functions as already reported in the field of lithium-ion batteries.[34, 40, 41]

3. Conclusion

The EC/DEC mixture, i.e. solvents often used in the field of lithium-ion batteries, was submitted to ionizing radiation that simulates an accelerated aging. Radiolysis provides the opportunity to study the reactivity of the mixture at very different time scales, ranging from picosecond to hours after irradiation. The decay of the electron in EC is ultrafast due to its attachment, leading to the formation of the radical anion. It is even faster than in PC, which can be attributed to less steric hindrance and to the absence of the methyl group that has an inductive electron donor effect. Nevertheless, the major channel for the formation of radical anions is thought to be the pre-solvated electron, which takes place on the femtosecond timescale. In the mixture, the formed electron is surrounded both by DEC and EC molecules. Once formed, it is very quickly trapped by EC molecules, leading to the formation of radical anions. Minutes and hours after irradiation, this implies that the amount of CO arising mainly from $EC^{\bullet -}$ will increase almost linearly with the EC electron fraction. Of course, this is not the case for H_2 and CH_4 whose origin is mainly DEC*. Lastly, the products detected both in the gas and liquid phases are consistent with the ones reported previously in electrochemistry experiments.

The present study evidences again the interest of using radiolysis to understand in details the behavior of solvents and electrolytes used in lithium-ion batteries.

Supporting Information: Products formed in the liquid phase after 100 kGy irradiation of the EC/DEC mixture and identified by High Resolution Mass Spectrometry (HRMS) experiments.

Acknowledgements

We would like to acknowledge CEA's DSM Energie program for funding. This work was also supported by a public grant from the "Laboratoire d'Excellence Physics Atom Light Mater" (LabEx PALM) overseen by the French National Research Agency (ANR) as part of

the “Investissements d’Avenir” program (reference: ANR-10-LABX-0039). Last, the authors want to thank Vincent Dauvois and Vincent Steinmetz for their help in the GC-MS and HRMS experiments.

Keywords

Lithium-ion battery; picosecond pulse radiolysis; radical ions; reaction mechanisms; steady-state radiolysis

References

[1] P. Poizot, F. Dolhem, *Energy Environ. Sci.* **2011**, *4*, 2003-2019.
[2] D. Larcher, J.M. Tarascon, *Nature Chem.* **2015**, *7*, 19-29.
[3] J.M. Tarascon, M. Armand, *Nature* **2001**, *414*, 359-367.
[4] K. Xu, *Chem. Rev.* **2004**, *104*, 4303-4417.
[5] S.F. Lux, I.T. Lucas, E. Pollak, S. Passerini, M. Winter, R. Kostecki, *Electrochem. Comm.* **2012**, *14*, 47-50.
[6] M. Metzger, B. Strehle, S. Solchenbach, H.A. Gasteiger, *J. Electrochem. Soc.* **2016**, *163*, A798-A809.
[7] M. Broussely, P. Biensan, F. Bonhomme, P. Blanchard, S. Herreyre, K. Nechev, R.J. Staniewicz, *J. Power Sources* **2005**, *146*, 90-96.
[8] G. Gachot, S. Grugeon, M. Armand, S. Pilard, P. Guenot, J.-M. Tarascon, S. Laruelle, *J. Power Sources* **2008**, *178*, 409-421.
[9] D. Ortiz, V. Steinmetz, D. Durand, S. Legand, V. Dauvois, P. Maître, S. Le Caër, *Nature Comm.* **2015**, *6*, 6950.
[10] D. Ortiz, I. Jimenez Gordon, J.-P. Baltaze, O. Hernandez-Alba, S. Legand, V. Dauvois, G. Si Larbi, U. Schmidhammer, J.L. Marignier, J.-F. Martin, J. Belloni, M. Mostafavi, S. Le Caër, *ChemSusChem* **2015**, *8*, 3605-3616.
[11] D. Ortiz, I. Jimenez Gordon, S. Legand, V. Dauvois, J.-P. Baltaze, J.L. Marignier, J.-F. Martin, J. Belloni, M. Mostafavi, S. Le Caër, *J. Power Sources* **2016**, *326*, 285-295.
[12] R.L. Naejus, D., R. Coudert, *J. Chem. Thermodynamics* **1997**, *29*, 1503-1515.
[13] D.S. Hall, J. Self, J.R. Dahn, *J. Phys. Chem. C* **2015**, *119*, 22322-22330.
[14] J. Belloni, H. Monard, F. Gobert, J.P. Larbre, A. Demarque, V. De Waele, I. Lampre, J.L. Marignier, M. Mostafavi, J.C. Bourdon, M. Bernard, H. Borie, T. Garvey, B. Jacquemard, B. Leblond, P. Lepercq, M. Omeich, M. Roch, J. Rodier, R. Roux, *Nucl. Instrum. Methods Phys. Res. A* **2005**, *539*, 527-539.
[15] U. Schmidhammer, A.K. El Omar, A. Balcerzyk, M. Mostafavi, *Rad. Phys. Chem.* **2012**, *81*, 1715-1719.
[16] U. Schmidhammer, P. Jeunesse, G. Stresing, M. Mostafavi, *Appl. Spectr.* **2014**, *68*, 1137-1147.
[17] Y. Muroya, M. Lin, G. Wu, H. Iijima, K. Yoshii, T. Ueda, H. Kudo, Y. Katsumura, *Rad. Phys. Chem.* **2005**, *72*, 169-172.
[18] H. Fricke, E.J. Hart, *Chemical Dosimetry*, in *Radiation Dosimetry*, F.H. Attix and W.C. Roesch, Editors. 1966, Academic press: New York and London. p. 167-232.
[19] F. Torche, A.K. El Omar, P. Babilotte, S. Sorgues, U. Schmidhammer, J.-L. Marignier, M. Mostafavi, J. Belloni, *J. Phys. Chem. A* **2013**, *117*, 10801-10810.

[20] M. Lin, H. Fu, I. Lampre, V. de Waele, Y. Muroya, Y. Yan, S. Yamashita, Y. Katsumura, M. Mostafavi, *J. Phys. Chem. A* **2009**, *113*, 12193-12198.
[21] S. Le Caër, D. Ortiz, J.L. Marignier, U. Schmidhammer, J. Belloni, M. Mostafavi, *J. Phys. Chem. Lett.* **2016**, *7*, 186-190.
[22] F.Y. Jou, L.M. Dorfman, *J. Chem. Phys.* **1973**, *58*, 4715-4723.
[23] W. Marbach, A.N. Asaad, P. Krebs, *J. Phys. Chem. A* **1999**, *103*, 28-32.
[24] A.E. Bragg, G.U. Kanu, B.J. Schwartz, *J. Phys. Chem. Lett.* **2011**, *2*, 2797-2804.
[25] P.K. Muhuri, D.K. Hazra, *J. Chem. Eng. Data* **1994**, *39*, 375-377.
[26] D. Ward, R. Jones, J. Templeton, K. Reyes, M. Kane, *ECS Trans.* **2014**, *61*, 181-191.
[27] D.M. Bartels, A.R. Cook, M. Mudaliar, C.D. Jonah, *J. Phys. Chem. A* **2000**, *104*, 1686-1691.
[28] M. Lin, M. Mostafavi, Y. Muroya, Z. Han, I. Lampre, Y. Katsumura, *J. Phys. Chem. A* **2006**, *110*, 11404-11410.
[29] L.M. Dorfman, F.-Y. Jou, *Optical Absorption Spectrum of the Solvated Electron in Ethers and in Binary Liquid Systems*, in *Electrons in Fluids*, J. Jortner and N.R. Kestner, Editors. 1973, Springer: New York.
[30] I.B. Martini, E. Barthel, B.J. Schwartz, *J. Chem. Phys.* **2000**, *113*, 11245-11257.
[31] M.J. Bedard-Hearn, R.E. Larsen, B.J. Schwartz, *J. Chem. Phys.* **2005**, *122*, 134506.
[32] M.J. Bedard-Hearn, R.E. Larsen, B.J. Schwartz, *J. Chem. Phys.* **2006**, *125*, 194509.
[33] M. Srilakshmi, T. Srinivasa Krishna, K. Narendra, R. Dey, A. Ratnakar, *J. Mol. Liquids* **2015**, *211*, 854-867.
[34] G. Gachot, P. Ribière, D. Mathiron, S. Grugeon, M. Armand, J.B. Leriche, S. Pilard, S. Laruelle, *Anal. Chem.* **2011**, *83*, 478-485.
[35] M. Metzger, J. Sicklinger, D. Haering, C. Kavakli, C. Stinner, C. Marino, H.A. Gasteiger, *J. Electrochem. Soc.* **2015**, *162*, A1227-A1235.
[36] V.I. Borovkov, *Phys. Chem. Chem. Phys.* **2017**, *19*, 49-53.
[37] B.B. Berkes, A. Schiele, H. Sommer, T. Brezesinski, J. Janek, *J. Solid State Electrochem.* **2016**, *20*, 2961-2967.
[38] J.W.T. Spinks, R.J. Woods, *An Introduction to Radiation Chemistry*. 3rd ed, Wiley-Interscience Publication: New York, USA, 1990.
[39] I.A. Shkrob, Y. Zhu, T.W. Marin, D. Abraham, *J. Phys. Chem. C* **2013**, *117*, 19255-19269.
[40] L. Gireaud, S. Grugeon, S. Pilard, P. Guenot, J.M. Tarascon, S. Laruelle, *Anal. Chem.* **2006**, *78*, 3688-3698.
[41] G. Gachot, S. Grugeon, M. Armand, S. Pilard, P. Guenot, J.-M. Tarascon, S. Laruelle, *J. Power Sources* **2008**, *178*, 409-421.